Short-range interactions between strongly nonlocal spatial solitons

Wei Hu,* Shigen Ouyang,* Pingbao Yang, Qi Guo,† and Sheng Lan
Laboratory of Photonic Information Technology, South China Normal University, Guangzhou 510631, People's Republic of China
and Laboratory of Light Transmission Optics, South China Normal University, Guangzhou 510631, People's Republic of China
(Received 1 June 2007; revised manuscript received 27 December 2007; published 24 March 2008)

Short-range interactions between strongly nonlocal spatial solitons were investigated and found to depend periodically on the soliton phase difference. Two solitons in close proximity can be intertrapped via the strong nonlocality, and propagate together as a whole. The trajectory of the propagation is a straight line with a slope controlled by the phase difference. Experimental results carried out in nematic liquid crystals agree quantitatively with the prediction. The modification of the Snyder-Mitchell model is also discussed. Our study suggests that the phenomenon in which optical beams can be steered by controlling the phase difference could be used in all-optical information processing.

DOI: 10.1103/PhysRevA.77.033842 PACS number(s): 42.65.Tg, 42.65.Jx, 42.70.Df, 42.70.Nq

I. INTRODUCTION

Solitons are a common phenomenon in many physical fields, while the interactions of the solitons have great potential in a wide range of applications [1]. The strongly nonlocal spatial soliton, which is also known as the accessible soliton [2] and is an optical beam self-trapped by a balance between diffraction and nonlinear propagation in nonlocal nonlinear media under the condition of strong nonlocality [3–5], has significant properties and has been of increasing interest in recent decades [2,6–9]. Several strongly nonlocal media, also referred to as highly nonlocal media in some literature (for example, Refs. [2,7,8]), have been found in experiments, such as nematic liquid crystal (NLC) [7–10], lead glass [11,12], thermal nonlinear liquid [13], and nonlinear ion gas [14]. Nonlocality is also found in photorefractive crystal [15,16], dipolar Bose-Einstein condensate [17,18], and quadratic nonlinear media [19].

The nonlocality of a nonlinear response may drastically modify the properties of solitons, especially their interactions. In a strongly nonlocal case, it has been shown theoretically and experimentally that attraction can occur between bright solitons with any phase difference [2,20–23], coherent or incoherent solitons [24,25], or dark solitons [13,26]. On the contrary, attraction occurs only for two in-phase local bright solitons [1]. Both long-range [12] and short-range interactions between solitons can occur in a strongly nonlocal nonlinearity, while only the short-range interaction can occur in a local nonlinearity because the force between the local solitons decreases exponentially with the separation between them [27].

It is well known that interactions between strongly nonlocal bright solitons are independent of their phase difference [2,12,20,21]. In this paper, we divide the interactions into two categories: short-range interactions and long-range interactions. We differentiate the patterns of short-range and long-range interactions between strongly nonlocal bright solitons, and show that the independence of the phase difference only holds for the long-range interaction. We show theoretically and experimentally that the short-range interaction of two strongly nonlocal bright solitons is periodically dependent on their phase difference.

In Sec. II, we give a theoretical description of the short-range interaction between nonlocal solitons derived from the conservation of momentum. We present numerical results and a modified phenomenological linearized model. Experiments using NLCs are reported in Sec. III. Section IV is the Conclusion.

II. THEORY OF THE INTERACTION IN STRONGLY NONLOCAL MEDIA

Let us consider a (1+2)-D model of a linearly polarized optical field with an envelope A propagating in the z direction in a medium with nonlocal nonlinearity as follows:

$$2ik\partial_z A + \nabla_\perp^2 A + 2k^2 \frac{\Delta n}{n_0} A = 0, \tag{1}$$

where $\nabla_\perp^2 = \partial_x^2 + \partial_y^2$ and k and n_0 are the wave-vector and linear refractive index of the medium. The nonlinear perturbation of the refraction index $\Delta n(x,y,z)$ can be generally expressed as

$$\Delta n = n_2 \int_{-\infty}^{\infty} R(x-x',y-y')|A(x',y',z)|^2 dx'dy', \tag{2}$$

where $R(x,y)$ is the real nonlinear response function of the medium. The normalized condition $\int_{-\infty}^{\infty} R(x,y)dxdy = 1$ is chosen physically such that the nonlinear index n_2 has the same dimensions as that in a local Kerr medium. If $R(x,y)$ is a delta function, $\Delta n = n_2|A|^2$ and Eq. (1) become the well-known nonlinear Schrödinger equations (NLSE) for the local Kerr medium. Equations (1) and (2), the so-called nonlocal nonlinear Schrödinger equations (NNLSE), can model the beam propagation in most nonlocal nonlinear media discovered by experiment so far.

For the NNLSE, several well-known invariant integrals are important for theoretical analysis [21,28]. The first is the beam power integral,

*These authors contributed equally to this work.
†guoq@scnu.edu.cn

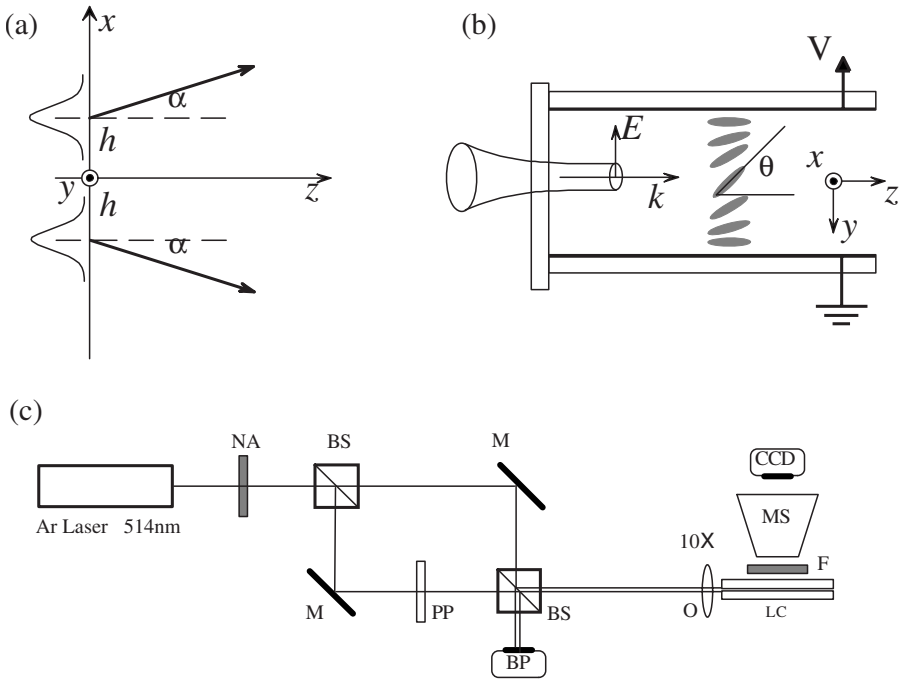

FIG. 1. Sketches of (a) the two injected solitons, (b) the liquid crystal cell, and (c) the experimental setup. NA, neutral attenuator; BS, beam splitters; *M*, plate mirror; PP, parallel-face plate for adjusting the phase difference; O, 10× microscope objective; LC, liquid crystal cell; MS, microscope; *F*, laser-line filter; and BP, beam profiler.

$$P = \int_{-\infty}^{\infty} |A(x,y)|^2 dxdy, \tag{3}$$

which results from the energy conservation of an optical beam during propagation in a lossless medium. If the nonlocal response function $R(x,y)$ is shift invariant and symmetric about its center, the spatial momentum

$$\vec{M} = \frac{1}{k}\int_{-\infty}^{\infty} A^*(-i\vec{\nabla}_\perp)Adxdy \tag{4}$$

is also a conserved quantity [21,28]. From Ehrenfest's theorem, we have

$$\frac{d\vec{r}_c(z)}{dz} = \frac{\vec{M}}{P}, \tag{5}$$

where

$$\vec{r}_c(z) = \frac{1}{P}\int_{-\infty}^{\infty} (x\hat{e}_x + y\hat{e}_y)|A(x,y,z)|^2 dxdy \tag{6}$$

is the trajectory of the mass center of the beam. Because $\vec{M}$ and P are conserved constants, from Eq. (5) we have

$$\vec{r}_c(z) = \frac{\vec{M}}{P}z + \vec{r}_{c0}, \tag{7}$$

where $\vec{r}_{c0}=\vec{r}_c(0)$. Equation (7) implies the trajectory of the mass center is a straight line with its slope with respect to the z axis determined by $\vec{M}/P$.

Suppose the two simultaneously incident Gaussian solitons are coplanar on the x-z plane, with a width w_0, a phase difference γ, and a separation $d(=2h)$, as shown in Fig. 1(a), i.e.,

$$A(x,y,0) = A_0 \exp\left[-\frac{(x+h)^2+y^2}{2w_0^2} + ik(x+h)\tan\alpha\right] + A_0 e^{i\gamma}\exp\left[-\frac{(x-h)^2+y^2}{2w_0^2} - ik(x-h)\tan\alpha\right], \tag{8}$$

where w_0 is the beam width, $2h$ is the initial separation between the two beams, γ is the initial phase difference between the two beams, α is the incident angle with respect to the z axis, and the amplitude A_0 is sufficiently large for the two beams to propagate in soliton states [2,7,8,20]. For the initial condition (8), we obtain the total beam power

$$P = 2\pi A_0^2 w_0^2 (1 + e^{-h^2/w_0^2 - k^2 w_0^2 \tan^2\alpha}\cos\gamma), \tag{9}$$

the spatial momentum

$$\vec{M} = M_x\vec{e}_x + M_y\vec{e}_y = \frac{2\pi h A_0^2}{k} e^{-h^2/w_0^2 - k^2 w_0^2 \tan^2\alpha}\sin\gamma\vec{e}_x, \tag{10}$$

and the initial position of the mass center $\vec{r}_{c0}=0$. Let β_x be the angle of the trajectory of the mass center with respect to the z axis; then the slope $\tan\beta_x = M_x/P$ is

$$\frac{\tan\beta_x}{\Theta} = \frac{(h/w_0)\exp[-(h/w_0)^2 - (\tan\alpha/\Theta)^2]\sin\gamma}{1+\exp[-(h/w_0)^2 - (\tan\alpha/\Theta)^2]\cos\gamma}, \tag{11}$$

and $\tan\beta_y=0$, where $\Theta = 1/kw_0$ is the far-field divergence angle of a Gaussian beam.

As shown in Fig. 2, the slope of the line for the trajectory of the mass center is highly dependent on the separation $2h$ and the phase difference γ, where we take $\alpha=0$, i.e., the two solitons are injected parallel into the medium. Figure 2 shows that $\tan\beta_x=0$ only when $\gamma=0$ or π for $h/w_0 \leq 2$, and $\tan\beta_x$ goes to zero when $h/w_0 \geq 2$. $\tan\beta_x$ has significant

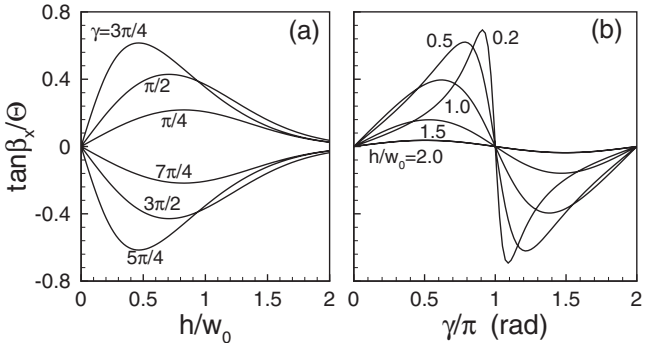

FIG. 2. Dependence of the slope on the distance h (a) and phase difference γ (b) for two parallel-injected solitons.

value when h is about or smaller than the beam width w_0. In other words, when the soliton separation $2h$ is approximately or larger than four times the soliton width w_0, the optical fields of the two solitons do not overlap and tan β_x decreases to zero; otherwise the two solitons have effective overlap and tan β_x has a nonzero value that changes with the phase difference.

It is important to emphasize that the above analytical result for the movement of the mass center [Eq. (11)] is universal and independent of the form of the nonlinear response function R. This means that no matter what the material, the degree of nonlocality, and the input power of the beams are, the movement of the mass center is the same as for the initial condition (8).

Although the momentum gives the movement of the mass center, it is difficult to obtain the analytical solution of the beam propagation for the initial condition (8). We carry out the numerical simulation for local, weakly nonlocal, and strongly nonlocal propagations, and only the (1+1)-D case for Eqs. (1) and (2) is simulated for the sake of simplicity and without the loss of generality. The (1+1)-D model makes it possible to compare propagations in nonlocal and local nonlinearity, and provides a sufficiently accurate description of (1+2)-D coplanar propagation. The results are shown in Fig. 3. The NLC is taken into consideration here for consistency with our experiment discussed later in this paper. The response function of the NLC is the exponential-decay function

$$R(x) = (1/2w_m)\exp(-|x|/w_w), \tag{12}$$

for the (1+1)-D case [21], and the zeroth-order modified Bessel function

$$R(x,y) = (1/2\pi w_m^2)K_0(\sqrt{x^2+y^2}/w_m), \tag{13}$$

for the (1+2)-D cylindrically symmetrical case [7,23], where w_m is the characteristic length of the response function R controlled by the bias voltage [23]. The ratio w_m/w_0 indicates the degree of nonlocality [3–5], which is chosen in the simulation to be 0.47 and 10 for the weakly nonlocal and strongly nonlocal cases in Fig. 3, respectively.

Some interesting consequences can be seen in Fig. 3. For the local system described by the NLSE, the two solitons attract only for the in-phase case (γ=0) and otherwise repel

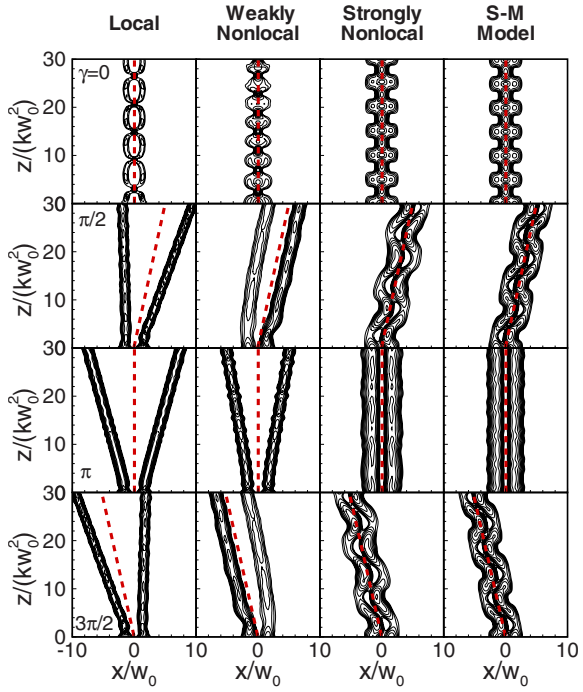

FIG. 3. (Color online) Contour graph of the numerical propagation of Eqs. (1) and (2) for the two parallel-injected solitons. The local case is shown in the first (from left to right) column, and the two different nonlocal cases with an exponential-decay response function given by Eq. (12) are shown in the second and third columns, respectively. The red dashed lines show the movement of the mass center of the two solitons. The results from the modified Snyder-Mitchell model, i.e., Eq. (17), with the same initial condition are presented in the fourth column for comparison. The phase differences between the two solitons are 0, $\pi/2$, π, and $3\pi/2$ (from top to bottom).

[1], while the mass center of the two solitons moves along straight lines with the slope determined by the initial momentum M_x. There is also a power transfer between the solitons when γ does not equal 0 or π, as mentioned in Ref. [1]. The force between the in-phase solitons is attractive and independent of the degree of nonlocality, as shown in the first row, whereas the repulsion between the solitons for the other phase difference cases weakens as the degree of nonlocality increases. As a result, two solitons with an arbitrary phase difference can attract when the nonlocality becomes sufficiently strong. For all of the propagations, however, the movement of the mass center obeys the same regulation, a straight-line trajectory with a slope given by Eq. (11). It is clear that for a strong enough nonlocality the two spatial solitons trap each other and propagate together as a whole along the trajectory of the mass center. Interestingly, a similar phenomenon was noted [29] in the intermediate process [30] for dealing with incoherent solitons in "fast" nonlocal nonlinear media.

It can be seen that the maximum value of the tilting angles occurs when γ approximates π for a small distance h (Fig. 4). For each value of h, β_x has extrema (a maximum and a minimum),

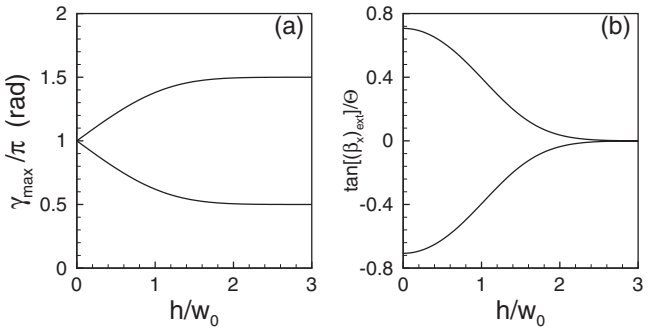

FIG. 4. (a) Phase difference γ_{max} for the maximum slope angle vs distance h, and (b) the maximum tilting angle $\tan[(\beta_x)_{ext}]$ vs distance h. $\alpha=0$ for both figures.

$$\frac{\tan(\beta_x)_{ext}}{\Theta} = \pm \frac{(h/w_0)\exp(-h^2/w_0^2)}{\sqrt{1-\exp(-2h^2/w_0^2)}} \tag{14}$$

at two values of γ_{max} between $\pi/2$ and $3\pi/2$, which are determined by

$$\cos\gamma_{max} = \pm\exp(-h^2/w_0^2). \tag{15}$$

The maximum is for steering right and the minimum for steering left. For smaller values of h, the tilt angle β_x is larger. The largest tilting angle is $\pm\Theta/\sqrt{2}$ when h approaches zero. Therefore, the steering angle of the whole beam is significant only for thin beams. For a typical beam with $w_0=5$ μm, the steering angle is only ± 0.01 rad.

From Figs. 2 and 3, when $d<4w_0$, the two solitons have a nonzero overlap and the slope $\tan\beta_x$ is nonzero. In this case, the two solitons can be intertrapped via the strong nonlocality, and propagate together as a whole with the diagonal trajectory of their mass center. This is the short-range interaction between the strongly nonlocal solitons, which is phase sensitive (controllable by their phase difference). When $d>4w_0$, on the other hand, the two solitons do not overlap and the slope of the trajectory of their mass center tends toward zero. In this case, the two strongly nonlocal solitons undergo periodic collisions in their coplanar propagation [2,12,20], or spiral about one another if they are initially unaligned [2,12]. Both processes have nothing to do with relative phase, as first predicted by Snyder and Mitchell [2] and then verified experimentally [12,20]. This is the long-range interaction between strongly nonlocal solitons. As the soliton separation d increases to become larger than $4w_0$, the interaction gradually changes from the short-range pattern to the long-range pattern in the strongly nonlocal nonlinearity, and vice versa. Only the short-range interaction, however, exists in the local nonlinearity [27].

It is worth noting that the Snyder-Mitchell model [2] cannot give a correct prediction for the short-range interaction between the strongly nonlocal solitons. The Snyder-Mitchell model [2]

$$2ik\frac{\partial A}{\partial z} + \nabla_\perp^2 A - \eta^2 r^2 A = 0 \tag{16}$$

was obtained under the supposition that $\vec{r}_c(z)\equiv 0$, which is equivalent to the supposition that both $\vec{M}=0$ and $\vec{r}_{c0}=0$. The model is valid only for the description of the short-range interaction between the in-phase and out-of-phase solitons, because the model requires inherent symmetry of the distribution of the optical field to ensure the symmetry of the nonlinear refractive index. As $\vec{M}$ approaches zero for the long-range interaction, the model is sufficiently accurate for all phase differences, and the long-range interaction is independent of the phase differences. If $\vec{M}|_{z=0}\neq 0$ or $\vec{r}_{c0}\neq 0$, however, the model will incorrectly predict that the mass center will have a sinusoidal motion for the short-range case. Since the momentum conservation is universal, a simple phenomenological modification can be made to include the movement of the mass center [Eq. (7)]

$$2ik\frac{\partial A}{\partial z} + \nabla_\perp^2 A - \eta^2\left(\vec{r} - \frac{\vec{M}}{P}z - \vec{r}_{c0}\right)^2 A = 0, \tag{17}$$

where $\vec{M}$ and $\vec{r}_{c0}$ are determined by Eqs. (4) and (6) according to the initial distribution of the optical field $A(\vec{r},0)$. By introducing the transformations

$$\vec{\rho} = \vec{r} - \frac{\vec{M}}{P}z - \vec{r}_{c0}, \tag{18}$$

$$\zeta = z, \tag{19}$$

and

$$\tilde{A}(\vec{\rho},\zeta) = A(\vec{r},z)\exp\left[-ik\frac{\vec{M}}{P}\cdot\left(\vec{\rho}+\frac{\vec{M}}{P}\zeta+\vec{r}_{c0}\right)+ik\frac{M^2}{2P^2}\zeta\right], \tag{20}$$

Eq. (17) becomes

$$2ik\frac{\partial\tilde{A}}{\partial\zeta} + \nabla_\perp^2\tilde{A} - \eta^2\rho^2\tilde{A} = 0. \tag{21}$$

The trajectory of the mass center of $\tilde{A}(\vec{\rho},\zeta)$ is a straight line along the ζ axis, and that of $A(\vec{r},z)$ is a straight line with a slope described by Eq. (5). Equation (21) is the same as Eq. (16), but they are for different coordinate systems. The reference frame for the Snyder-Mitchell model is at rest (a laboratory coordinate system), while the reference frame for Eq. (21) [or Eq. (17)] moves with the mass center. In this sense, Eq. (21) [or Eq. (17)] can be called a modified Snyder-Mitchell model. When both $\vec{M}=0$ and $\vec{r}_{c0}=0$, the modified Snyder-Mitchell model reduces to the Snyder-Mitchell model. It is easy to prove that momentum is conserved for the modified Snyder-Mitchell model [Eq. (17)]. The derivation of Eq. (17) from the phenomenological NNLSE and its analytical solution for the interaction of two Gaussian beams have been presented in Ref. [31]. The results of Eq. (17) are shown in the fourth column of Fig. 3 as a comparison with the third column. The parameter η is chosen according to the corresponding period in the third column.

III. EXPERIMENT USING NLC

To verify our prediction, we carried out an experiment on NLC. The configuration of the NLC cell is the same as in

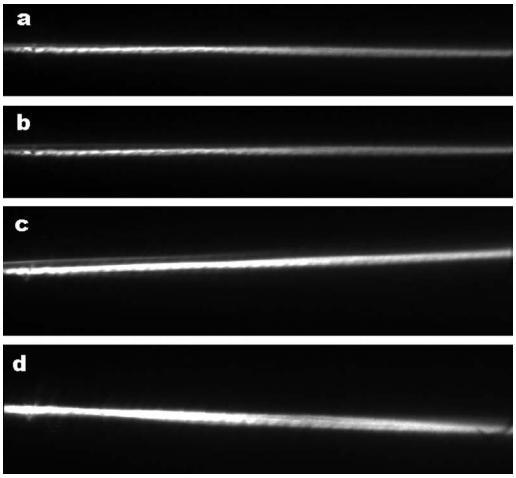

FIG. 5. Photos of the beam trajectories for the single soliton [(a) and (b)] and the two solitons injected together [(c) and (d)] propagating in the NLC cell. The phase differences between the two solitons for (c) and (d) are about $\pi/2$ and $3\pi/2$, respectively.

previous works [8,10,23], and is shown in Fig. 1(b). The optical field polarized along the y axis with an envelope A propagates in the z direction. An external low-frequency bias voltage V is applied in the y direction to control the initial tilt angle of the NLC. The evolution of the paraxial beam A and tilt angle θ are described by the equations in Refs. [7,32].

The experimental setup is illustrated in Fig. 1(c). The beam from the laser is split into two beams that are combined with a small separation by a second beam splitter and launched into a 80-μm-thick NLC cell by a 10× microscope objective. The beam width at the focus w_0, separation d, and relative angle 2α between the two beams are measured by an edged-scanning beam profiler with the NLC cell removed. The cell is filled with NLC TEB30A (from Slichem China Ltd.), for which $n_{\parallel}=1.6924$, $n_{\perp}=1.5221$, $K\approx 10^{-11}N$, $\epsilon_a^{\mathrm{op}}=0.5474$, and $\epsilon_a^{RF}=9.4$. The bias voltage on the cell is set to 1.4 V and the pretilt angle is nearly $\pi/4$ to obtain a sufficiently strong nonlocality and the lowest critical power for the solitons [22,23]. The launching power for each beam is fixed to 6 mW, and two spatial solitons are obtained for such excitation. The parameters for the beams inside the NLC are calculated from the measurement without the NLC cell, i.e., $w_0=2.2$ μm, $2h=2.25$ μm $(h/w_0=0.51)$, $\tan(2\alpha)=0.0076$, and the divergence angle $\Theta=0.0231$.

The phase difference between the two beams (solitons) is adjusted by the rotation of a 1.8-mm-thick parallel-face plate, and measured via its interference pattern by the beam profiler located on the other branch after the second beam splitter. First we find the position of the plate while the phase difference is adjusted to zero (in phase), then we rotate the plate in small steps to increase the phase difference γ.

Soliton trajectories are recorded by a charge coupled device (CCD) camera, as shown in Fig. 5. In Figs. 5(a) and 5(b), each of two solitons is launched alone into the NLC cell, and their trajectories are found to be straight and horizontal. When two solitons are injected simultaneously into the cell, they propagate as a whole, and tilt up [Fig. 5(c)] or down [Fig. 5(d)] in the x direction. Since the separation is so small that two solitons cannot be distinguished by the microscope in our experiment, we see a whole beam, as a bound state, steered by the phase difference γ.

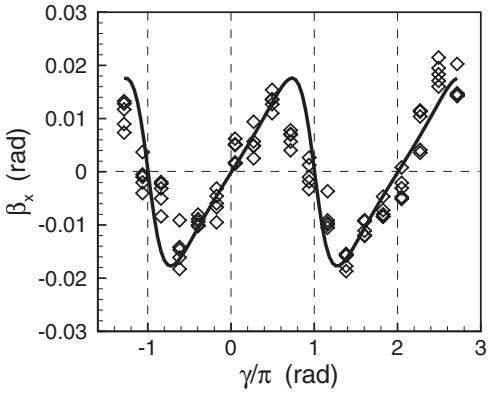

FIG. 6. Tilting angle of two beams vs the phase difference between them. Square points, experiment results; solid curve, the theoretical fitting from Eq. (11).

To compare quantitatively our experimental observation with our theoretical prediction, we vary the tilting angle with the phase difference γ as seen in Fig. 6. For each value of γ, we take five photographs of the beam to show the scatter of the tilting angle resulting from the variability of the laser source and the phase difference. The tilting angle for each photograph is plotted in Fig. 6 and the theoretical prediction is shown as the solid line. We can see that the experimental points locate around the theoretical prediction with a relatively small random error. The error is mainly due to the slight variations in the phase difference γ. Except for these random errors, we can say the experimental results are very consistent with the theoretical prediction. The maximum tilting angle observed in the experiment is about 1.2°, or approximately 0.6Θ.

IV. CONCLUSION AND DISCUSSION

We studied the short-range interaction between strongly nonlocal solitons and found the interaction strongly depends on the solitons' phase difference. The result is universal and independent of the nonlocal nonlinear media. An experiment carried out in NLC agrees quantitatively with the prediction. The Snyder-Mitchell model can only correctly predict the long-range interaction between strongly nonlocal solitons, whereas the modified Snyder-Mitchell model can correctly predict both long-range and short-range interactions between the solitons.

Unlike their local counterparts, the strongly nonlocal solitons can exhibit both short-range and long-range interactions. The two kinds of interactions, however, have different patterns; the former is phase sensitive and the latter is not. Therefore, both phenomena provide a means of controlling light with light and thus have potential in developing all-optical signal processing devices. They will, of course, be applied in different situations.

In addition, angular momentum is another invariant integral for the general NNSLE. Recently, Fratalocchi *et al.* studied the conservation of angular momentum for the rotation of a two soliton cluster in NLC theoretically and experimentally [33,34]. The analysis of angular momentum by Fratalocchi *et al.*, and in the present study, are similar but the interaction properties are different.

ACKNOWLEDGMENTS

This work was supported by the National Natural Science Foundation of China (Grant No. 10674050) and the Program for Innovative Research Teams in Higher Education in Guangdong (Grant No. 06CXTD005). The authors would like to thank Professor Li Xuan for her supply of the NLC cell samples.

[1] G. I. Stegeman and M. Segev, Science **286**, 1518 (1999), and references therein.
[2] A. W. Snyder and D. J. Mitchell, Science **276**, 1538 (1997).
[3] W. Krolikowski and O. Bang, Phys. Rev. E **63**, 016610 (2000).
[4] Q. Guo, B. Luo, and S. Chi, Opt. Commun. **259**, 336 (2006).
[5] Q. Guo, B. Luo, F. Yi, S. Chi, and Y. Xie, Phys. Rev. E **69**, 016602 (2004).
[6] A. S. Desyatnikov, A. A. Sukhorukov, and Y. S. Kivshar, Phys. Rev. Lett. **95**, 203904 (2005).
[7] C. Conti, M. Peccianti, and G. Assanto, Phys. Rev. Lett. **91**, 073901 (2003).
[8] C. Conti, M. Peccianti, and G. Assanto, Phys. Rev. Lett. **92**, 113902 (2004).
[9] M. Peccianti, C. Conti, G. Assanto, A. De Luca, and C. Umeton, Nature (London) **432**, 733 (2004).
[10] M. Peccianti, A. De Rossi, G. Assanto, A. De Luca, C. Umeton, and I. C. Khoo, Appl. Phys. Lett. **77**, 7 (2000).
[11] C. Rotschild, O. Cohen, O. Manela, M. Segev, and T. Carmon, Phys. Rev. Lett. **95**, 213904 (2005).
[12] C. Rotschild, B. Alfassi, O. Cohen, and M. Segev, Nat. Phys. **2**, 769 (2006).
[13] A. Dreischuh, D. Neshev, D. E. Petersen, O. Bang, and W. Królikowski, Phys. Rev. Lett. **96**, 043901 (2006).
[14] D. Suter and T. Blasberg, Phys. Rev. A **48**, 4583 (1993).
[15] M. Segev, B. Crosignani, A. Yariv, and B. Fischer, Phys. Rev. Lett. **68**, 923 (1992).
[16] W. Królikowski, M. Saffman, B. Luther-Davies, and C. Denz, Phys. Rev. Lett. **80**, 3240 (1998).
[17] A. Parola, L. Salasnich, and L. Reatto, Phys. Rev. A **57**, R3180 (1998).
[18] A. Griesmaier, J. Werner, S. Hensler, J. Stuhler, and T. Pfau, Phys. Rev. Lett. **94**, 160401 (2005).
[19] N. I. Nikolov, D. Neshev, O. Bang, and W. Z. Królikowski, Phys. Rev. E **68**, 036614 (2003).
[20] M. Peccianti, K. Brzdakiewicz, and G. Assanto, Opt. Lett. **27**, 1460 (2002).
[21] P. D. Rasmussen, O. Bang, and W. Królikowski, Phys. Rev. E **72**, 066611 (2005).
[22] M. Peccianti, C. Conti, and G. Assanto, Opt. Lett. **30**, 415 (2005).
[23] W. Hu, T. Zhang, Q. Guo, L. Xuan, and S. Lan, Appl. Phys. Lett. **89**, 071111 (2006).
[24] M. Peccianti, and G. Assanto, Phys. Rev. E **65**, 035603(R) (2002).
[25] M. Shen, Q. Wang, J. Shi, Y. Chen, and X. Wang, Phys. Rev. E **72**, 026604 (2005).
[26] N. I. Nikolov, D. Neshev, W. Królikowski, O. Bang, J. J. Rasmussen, and P. L. Christiansen, Opt. Lett. **29**, 286 (2004).
[27] J. P. Gordon, Opt. Lett. **8**, 596 (1983).
[28] A. I. Yakimenko, V. M. Lashkin, and O. O. Prikhodko, Phys. Rev. E **73**, 066605 (2006).
[29] O. Cohen, H. Buljan, T. Schwartz, J. W. Fleischer, and M. Segev, Phys. Rev. E **73**, 015601(R) (2006).
[30] In Ref. [29], the propagation of incoherent solitons in "fast" nonlocal nonlinear media was studied in two steps: (1) analyzing the propagation within a very short time interval (a time frame much shorter than the characteristic fluctuation time) during which the beam can be treated as a coherent speckled wave, and (2) calculating the propagation of the time-averaged envelope. In the intermediate process (step 1), it is found possible to steer intertrapped solitons by controlling their phase difference. After step 2, however, such phase sensitivity is lost for the time-averaged envelope.
[31] S. Ouyang, W. Hu, and Q. Guo, Phys. Rev. A **76**, 053832 (2007).
[32] M. Peccianti, C. Conti, G. Assanto, A. De Luca, and C. Umeton, J. Nonlinear Opt. Phys. Mater. **12**, 525 (2003).
[33] A. Fratalocchi, A. Piccardi, M. Peccianti, and G. Assanto, Opt. Lett. **32**, 1447 (2007).
[34] A. Fratalocchi, A. Piccardi, M. Peccianti, and G. Assanto, Phys. Rev. A **75**, 063835 (2007).